Draft version December 1, 2023
Typeset using LaTeX **twocolumn** style in AASTeX631

The Light Curve Measurement of Z Draconis by DoA Dome Telescope

Jin Bingcheng[1]

[1]*Department of Astronomy, School of Physics, Peking University, Beijing 100871, China*

ABSTRACT

I present the data reduction process and final results for DoA Dome Telescope observations for several variables during few nights in September. These data consist of Optical imaging in three broadband filters (B, V, sdss-r) over all pointings. I reduced the imaging data with a self-bulit Calibration Pipeline, with custom modifications and reduction steps designed to address additional features and challenges with the data. Here I provide a detailed description of each step in my reduction and a discussion of final measurement results. The final results are light curves for Z Draconis in each filter. I compare my data with previous measurement and the result shows consistentency.

Keywords: Variables, Imaging, Data Reduction, WCS Calibration, Flux Calibration, Optical Light Curve

1. INTRODUCTION

In September 2023, the class OBS 2023 used DoA Dome telescope to observe several variables. The observing schedule includes SX Phe Variable CY Aqr, RR Lyrae Variable XZ Cyg, SW And, and Eclipsing Binary U Sge, Z Dra. The scientific goal of this observation is to measure the light curve of these variables in different filters. To achieve this goal, My report is structured as follows. In Section 2, I will describe the observation and data acquisition. In Section 3, I present my own data reduction process, which is a custom pipeline for image reduction. In Section 4, I will point out the known issues in the data reduction. In Section 5, the final results is presented. In Section 6, I will finally discuss the results and comparison with previous measurement.

2. DOA DOME TELESCOPE OBSERVATIONS

The DoA Dome Telescope is a 40cm telescope located at DoA Dome Observatory in Peking University, Beijing, China. The detector is a 36mm×24mm QHY-11 CCD with 9um pixels, giving a field of view of approaximately 30×20 square arcmins. The data consist of Optical imaging in three broadband filters (B, V, sdss-r) over all pointings. For time-series observations, we have multiple exposures at different time epoch for each sources. The observation log is shown in Appendix 2.

3. IMAGE REDUCTION

3.1. *Stage1 – Detector-level Corrections*

Stage 1 of my Calibration Pipeline performs detector-level corrections, many of which are common to all instruments and observing modes. This stage of reduction take care of instrumental contaminations on the CCD chip, including bias, dark, and flat field corrections.

3.1.1. *Bias Subtraction*

For every single image taken by the CCD, there is a bias level that is added to the image. This bias level is a result of the CCD electronics and is independent of the exposure time (might be influenced by the temperature of the electronics). The bias level is measured by taking a zero-length exposure, which is an exposure with zero exposure time. The bias level is then subtracted from every image taken by the CCD. This step is actually done by Professor Wang Ran, and I just use the bias subtracted images in the following steps.

3.1.2. *Dark Subtraction*

Dark subtraction is a process that removes the dark current from the CCD. The dark current is a result of thermal electrons in the CCD that are generated by the heat of the CCD. The dark current is measured by taking a series of exposures with the same exposure time as the science images, but with the shutter closed. This step is again done by Professor Wang Ran, and I just use the dark frame for each exposure time to subtract the dark current from the science images.

3.1.3. *Flat Correction*

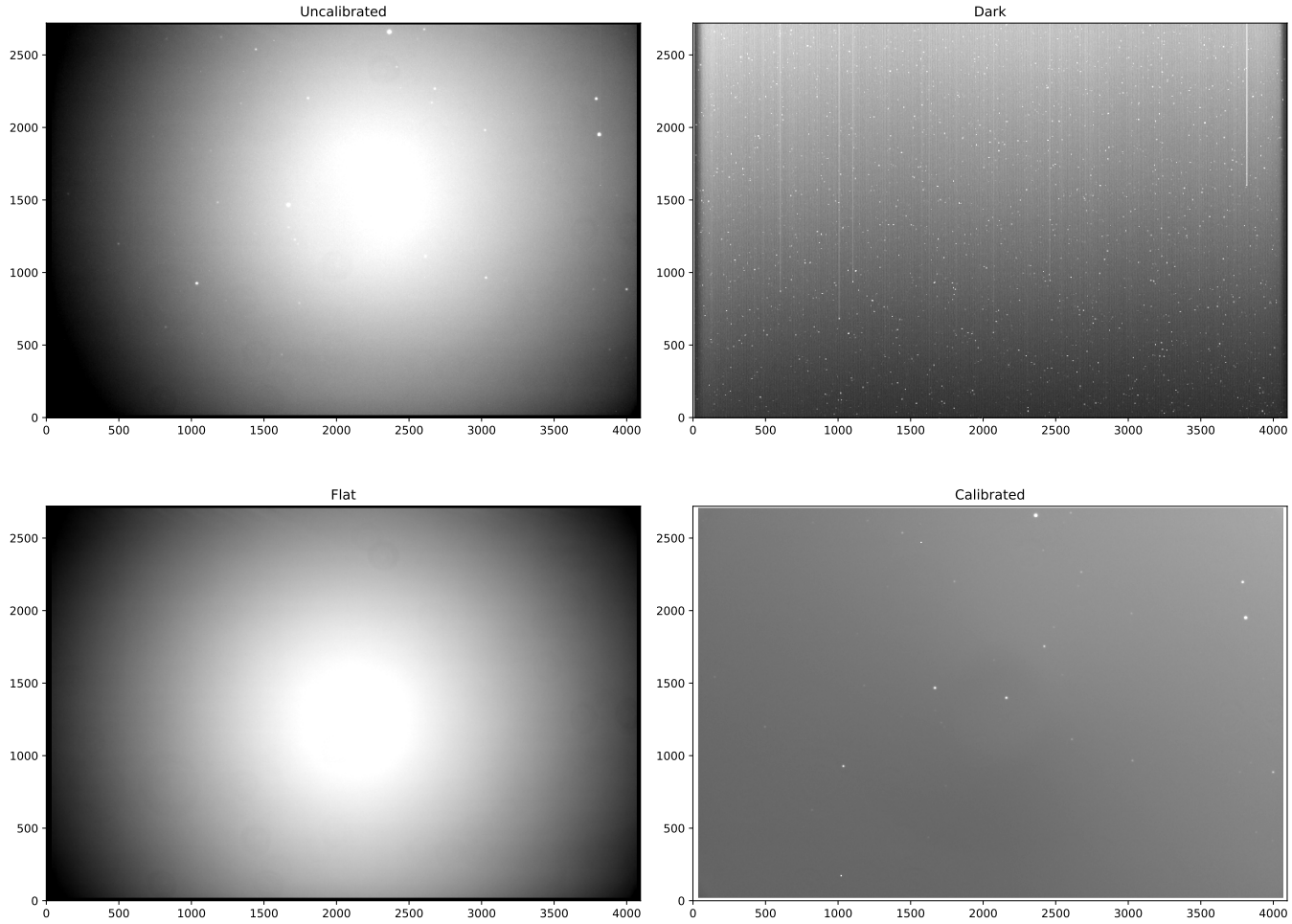

Figure 1. The result of stage 1 reduction. The upper left panel shows the bias subtracted raw image, and the upper right panel shows the 50s dark image provided by Prof. Wang Ran. The lower left panel shows the normalized flat field image again from Prof. Wang Ran, and the lower right panel shows the final calibrated image.

Flat correction is a process that corrects for pixel-to-pixel sensitivity variations across the CCD. The flat correction is performed by dividing each image by a normalized flat field image. Again here, the flat field image is provided by Professor Wang Ran, with dark and bias subtracted. The flat field image is normalized by dividing the median value of the image. The science images are then divided by the normalized flat field image, directly after the dark subtraction step. Figure 1 shows the result of stage 1 reduction.

3.2. *Stage2 – Individual Image Calibrations*

Stage 2 of my Calibration Pipeline performs calibrations that are specific to individual images. These calibrations are performed on each image independently of all other images.

3.2.1. *Source Detection*

Source detection is a pre-process for astrometric calibration and flux calibration. The source detection is performed by using the DAOStarFinder, which is a Python package in Photutils[1]. The DAOStarFinder is a source detection algorithm that uses a 2D Gaussian function to fit the sources in the image (Stetson 1987). Considering the fact that stars in the image are not perfect point sources due to PSF and most importantly, the seeing effect, I set the FWHM of the DAOStarFinder input to be 14 pixels, which is approximately the FWHM of the stars in the image revealed by software SAOImageDS9. However, since the seeing is not constant during the observation among different nights, the choice of FWHM, should be under careful consideration. 14 pix-

[1] https://photutils.readthedocs.io/en/stable/

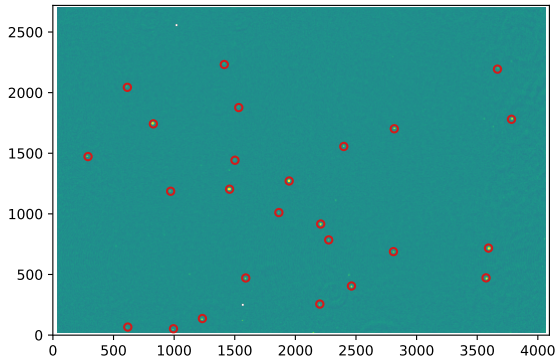

Figure 2. The result of source detection. The red circles show the sources detected by DAOStarFinder. The result shows that the FWHM of the stars in the image is approximately 14 pixels.

els is proved to be a good choice by the result of source detection shown in Figure 2.

The detection threshold is set to be 5σ above the background estimated by the mean or mode estimator depending on crowdness of the field. If the field is crowded, the mode estimator is used, otherwise the mean estimator is used. The background rms is estimated by the standard deviation after sigma-clipping.

3.2.2. *Astrometric Calibration*

Astrometric calibration is a process that converts the pixel coordinates of sources in the image to the sky coordinates (RA, Dec). The astrometric calibration is performed by using the astrometry.net[2] package. With the source catalog at hand, the astrometry.net package will match the sources with given initial parameters and return the wcs solution. To test the accuracy of the astrometric calibration, I crossmatch the sources with the reference catalog from the American Association of Variable Star Observers (AAVSO). More details will be described in Section 3.3.2.

3.3. *Stage3 – Ensemble Processing*

Stage 3 of my Calibration Pipeline performs science-level calibrations to ensemble images. These calibrations are performed on all available images together, and are therefore able to take advantage of the statistical properties of the ensemble.

3.3.1. *Drizzle*

After assigning WCS information to individual images, I am able to combining 'dithered' images into a single image. The reason I use the phrase 'dithered' is because the images are not dithered intentionally, but the telescope is not tracking the target perfectly, so the images are dithered unintentionally, which, however, is good for combining images. Drizzle is a linear reconstruction of an image from undersampled, dithered data. It can weight input images according to the statistical significance of each pixel, and removes the effects of geometric distortion both on image shape and photometry (Fruchter & Hook 2002). The combining process is performed by using the Drizzle package powered by Astropy. The drizzle package is able to combine images with different pixel scales and orientations. This step is necessary because the image quality is heavily defected by CCD defects and seeing effect. The final image is shown in Figure 3. The image shows that the image quality is improved after drizzling, including the removal of bad pixels and the improvement of the signal-to-noise ratio.

3.3.2. *Crossmatch*

To calibrate physical properties of the sources in the image, I need to crossmatch the sources with the reference catalog from APASS. The AAVSO Photometric All-Sky Survey (APASS, Henden et al. (2018)) performed an allsky photometric survey in 5 filters: Johnson B and V, sdss-g, sdss-r and sdss-i. Since APASS has the same filters as our observation, it should be a good reference catalog for our observation.

I do not use source detected from the individual images from the previous step 3.2.1 because the image quality is not satisfying. Instead, I use the source detected from the drizzled image.

The crossmatch is performed by using the Astropy[3] package. The final crossmatch result is shown in Figure 4. The distribution shows that the separation between the sources in the image and the reference catalog is less than 1.6 arcsec, indicating a satisfying astrometric calibration, even after drizzling.

3.3.3. *Flux Calibration*

Flux calibration is a process that converts the instrumental magnitude of sources in the image to the calibrated magnitude. The flux calibration is performed by using the aperture photometry method. The aperture photometry is measured based on the source detection step which is described in Section 3.2.1.

[2] https://astrometry.net/

[3] http://www.astropy.org

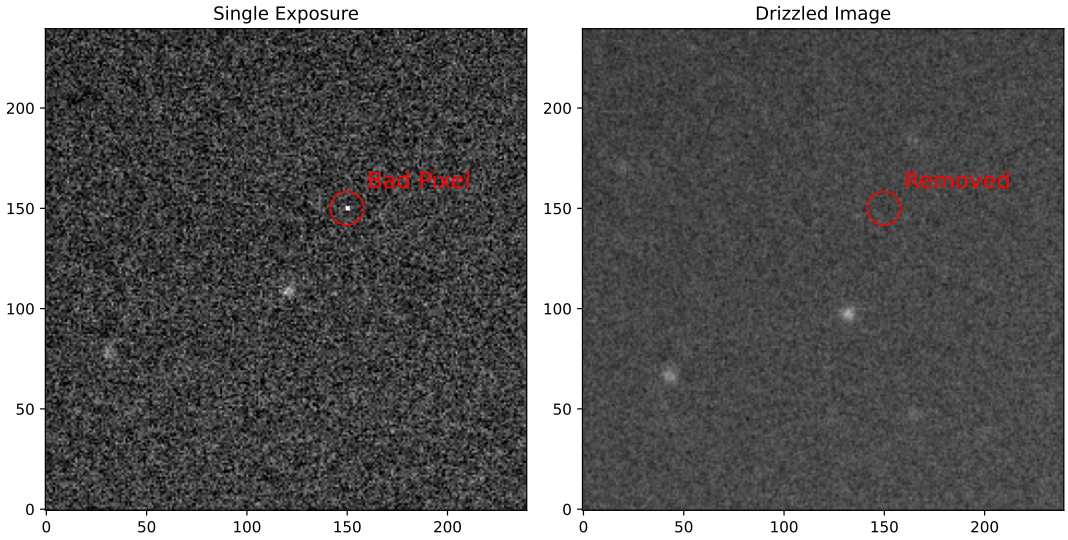

Figure 3. The result of drizzle. The left panel shows the raw image before drizzle, and the right panel shows the image after drizzle. The image quality is improved after drizzle, including the removal of bad pixels and the improvement of the signal-to-noise ratio.

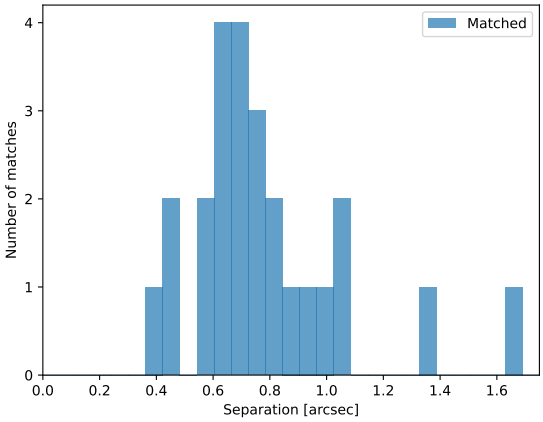

Figure 4. The distribution of separation between sources and the reference catalog. There are totally 25 number of matches (including the target variable). Most matches are within 1.0 arcsec, and the maximum separation is below 1.6 arcsec.

For convenience of comparing, I choose to measure the total magnitude of the sources in the image. However, the aperture radius should be chosen carefully because the image quality is heavily defected by the seeing effect and drizzling with inaccurate WCS information. The aperture radius has to be large enough to include most of the flux from the source, but not too large to include the flux from neighboring sources. After several tests, I choose the aperture radius to be 22.0 arcseconds because the field is not crowded.

After selecting the aperture, I then measure the aperture photometry with circular annulus to subtract the

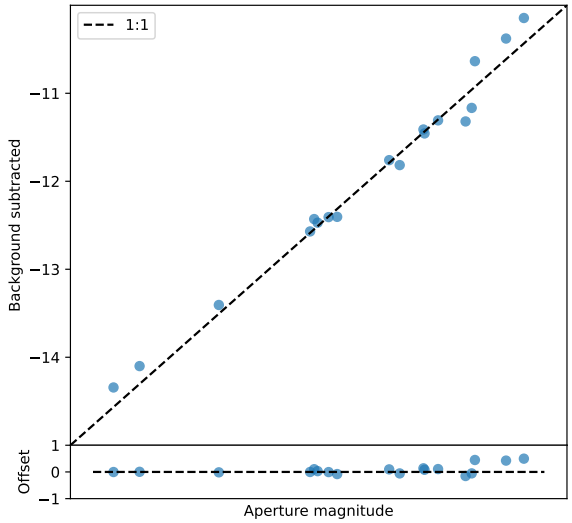

Figure 5. The background subtraction. The result shows that the local background is not well subtracted from the global background estimation, especially for faint stars.

local background. This step Turns out to be very important because the local background is not well subtracted from the global background estimation, as shown in Figure 5.

With a robust aperture photometry, I calibrate the zeropoint by regressing the instrumental magnitude with the reference catalog. The calibration of band sdss-r magnitude is based on catalog downloaded from SDSS. The calibration of band B and V magnitude is based on

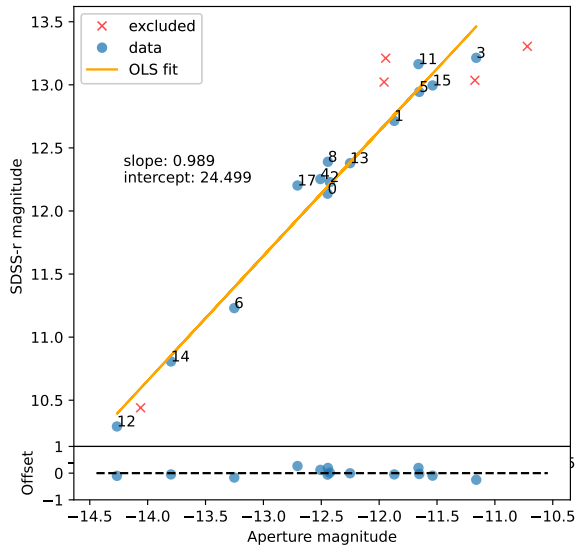

Figure 6. The V band zeropoint calibration. After removing several outliers, the slope of the regression line is very close to 1, and the linear model is statistically significant with a p-value of 0.000, suggesting a satisfying zeropoint calibration.

catalog provided by APASS. The variable itself cannot be used to calibrate the zeropoint.

An example of Flux calibration is shown in Figure 6, after removing several outliers, I derive the zeropoint in B and V band at different epoch respectively. However, the zeropoint in sdss-r band is not robust because the slope somehow cannot reaches 1. I will leave this problem to section 4.2. The final calibrated magnitude is shown in table 1. From the table we can see that the zeropoint is varying from epoch to epoch, which is reasonable because the airmass is varying from epoch to epoch. There is still a systematic difference between the zeropoint in B and V band, which is easy to understand. The zeropoint error is quite large, which is probably due to the limited number of reference stars.

4. KNOWN ISSUES

4.1. *Error Budget*

The error of photometry cannot be calculated directly from the science data. I need to construct an error map for science image with not only science frame itself, but flat frame, dark frame and bias frame as well. However, since I cannot obtain the readnoise from the detector, it's hard to only construct the error map with the poisson noise. And the error will propogate during the calibration process including drizzling.

Table 1. Zeropoint calibration results

Epoch (MJD)	Band	zeropoint (mag)	zeropoint error (mag)
60214.8227	V	24.3224	1.1648
60214.8457	V	24.3495	1.2692
60214.8763	V	24.3304	1.1865
60214.9095	V	24.3058	0.6174
60214.8249	B	24.4985	0.6025
60214.8495	B	24.4497	0.4634
60214.8786	B	24.4773	0.9179
60214.9117	B	24.5359	0.6232

4.2. *Flux calibration in sdss-r band*

When I try to calibrate the zeropoint in sdss-r band, I find that the slope of the regression line is not close to 1, as shown in Appendix B. Under the circumstance, I choose not to present the calibrated magnitude in sdss-r band in the final result.

5. RESULTS

5.1. *Light Curve Measured by DoA Dome Telescope*

The Class OBS 2023 has observed Z Dra in 4 different time epochs, and each time epoch has 3 different filters and multiple exposures. The light curve is finally measured by the drizzled image at each time epoch. The

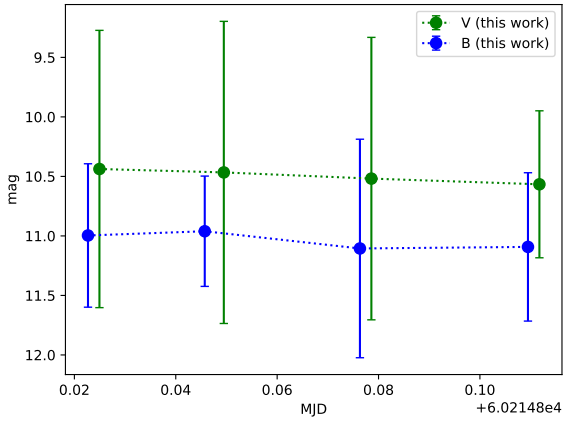

Figure 7. The light curve of Z Dra measured by DoA Dome Telescope. There is slightly an evidence of variable in the light curve, which will be explained in the next section 6.1

result is shown in Figure 7. There is a slight trend that the variable is getting dimmer from the first epoch to the last epoch. This could indicate a start of eclipse, as discussed in section 6.1.

6. DISCUSSION

6.1. *Light Curve of Z Draconis*

Combining with results from Terrell & Nelson (2017), I plot the complete light curve of Z Draconis in Figure 8. The orbital period of Z Draconis is 1.53 days according to Terrell & Nelson (2017), and the result is shifted to a single period. The result shows that the light curve measured by DoA Dome Telescope is consistent with the previous measurement. However, the light curve measured by DoA Dome Telescope is not spanning enough time to cover the whole period of Z Draconis. This is quite unfortunate because most of the eclipsing time is missing. I cannot drive any conclusion and constraints on the physical nature of Z Draconis from our DoA Dome measurement.

Thank Professor Wang Ran for providing the data and some of the first stage reduction product.

Facilities: DoA Dome Telescope

Software: astropy (Astropy Collaboration et al. 2013), photutils (Bradley et al. 2023), astrometry.net Lang et al. (2010)

APPENDIX

A. OBSERVATION LOG

The observation log is shown in Table 2.

B. SDSS-R FLUX CALIBRATION RESULTS

There is a systematic deviation from the APASS catalog in sdss-r band, as shown in Figure 9. The measurement from DoA Dome Telescope is systematically fainter than the APASS catalog. The reason is unknown, but I suspect that the catalog from APASS is not accurate enough.

To prove that, I do flux calibration in sdss-r band by using the catalog from SDSS. The result is shown in Figure 10. However, since I only have limited samples, I am not able to draw any conclusion. I will leave this problem aside because B and V band data is sufficient.

Table 2. Observation Log

Object	Filter	Exposure Time (s)	Number of Exposures	Date	Time
Z Dra	B	50	3	2023-09-27	19:44:40
Z Dra	V	50	3	2023-09-27	19:47:55
Z Dra	sdss-r	50	3	2023-09-27	19:51:11
Z Dra	B	50	5	2023-09-27	20:17:50
Z Dra	V	50	5	2023-09-27	20:23:15
Z Dra	sdss-r	50	5	2023-09-27	20:30:50
Z Dra	B	50	3	2023-09-27	21:01:55
Z Dra	V	50	3	2023-09-27	21:05:10
Z Dra	sdss-r	50	3	2023-09-27	21:08:26
Z Dra	B	50	3	2023-09-27	21:49:39
Z Dra	V	50	3	2023-09-27	21:52:54
Z Dra	sdss-r	50	3	2023-09-27	21:58:19

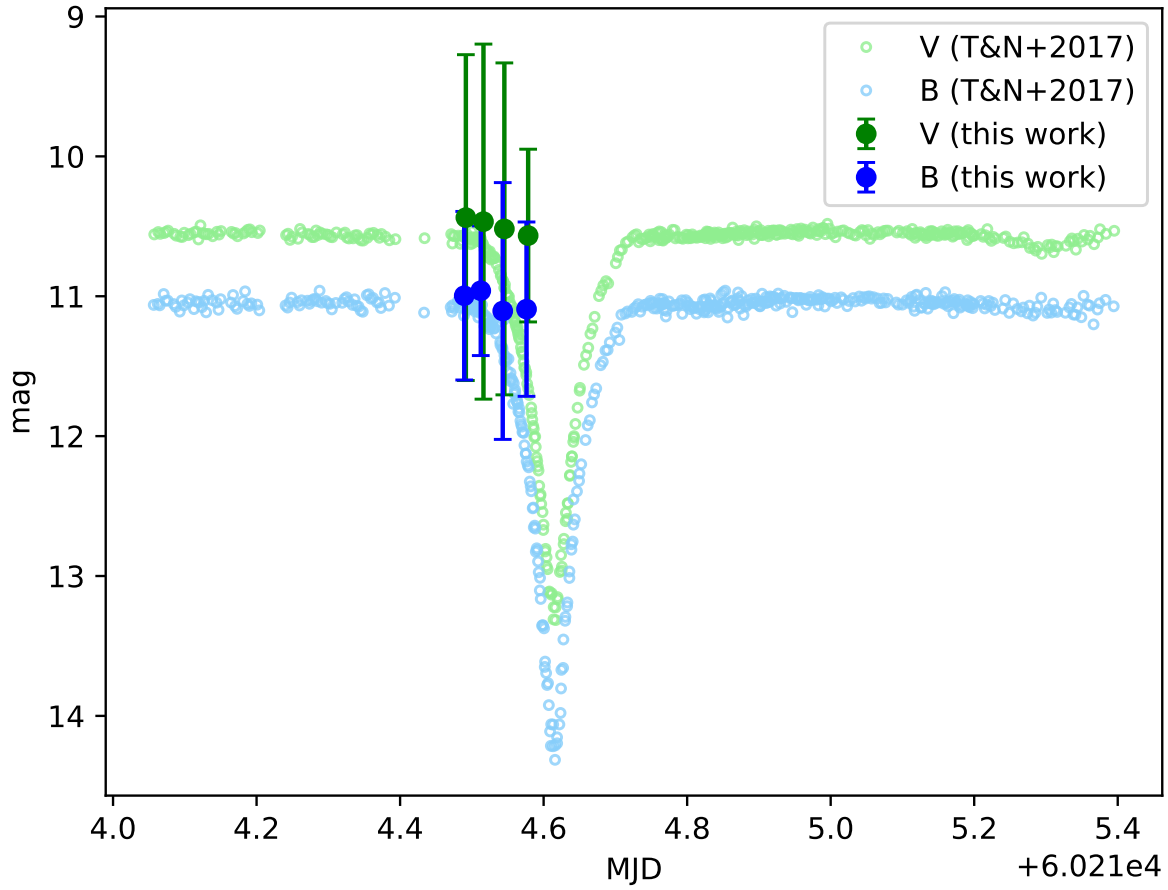

Figure 8. The light curve of Z Draconis. The blue curve shows the light curve measured by DoA Dome Telescope, and the red curve shows the light curve measured by Terrell & Nelson (2017).

REFERENCES

Astropy Collaboration, Robitaille, T. P., Tollerud, E. J., et al. 2013, A&A, 558, A33, doi: 10.1051/0004-6361/201322068

Bradley, L., Sipőcz, B., Robitaille, T., et al. 2023, astropy/photutils: 1.10.0, 1.10.0, Zenodo, doi: 10.5281/zenodo.1035865

Fruchter, A., & Hook, R. 2002, Publications of the Astronomical Society of the Pacific, 114, 144–152, doi: 10.1086/338393

Henden, A. A., Levine, S., Terrell, D., et al. 2018, AAVSO Photometric All Sky Survey (APASS) DR10, VO resource provided by the GAVO Data Center. http://dc.zah.uni-heidelberg.de/apass/q/cone/info

Lang, D., Hogg, D. W., Mierle, K., Blanton, M., & Roweis, S. 2010, The Astronomical Journal, 139, 1782–1800, doi: 10.1088/0004-6256/139/5/1782

Stetson, P. B. 1987, PASP, 99, 191, doi: 10.1086/131977

Terrell, D., & Nelson, R. H. 2017, Information Bulletin on Variable Stars, 6223, 1, doi: 10.22444/IBVS.6223

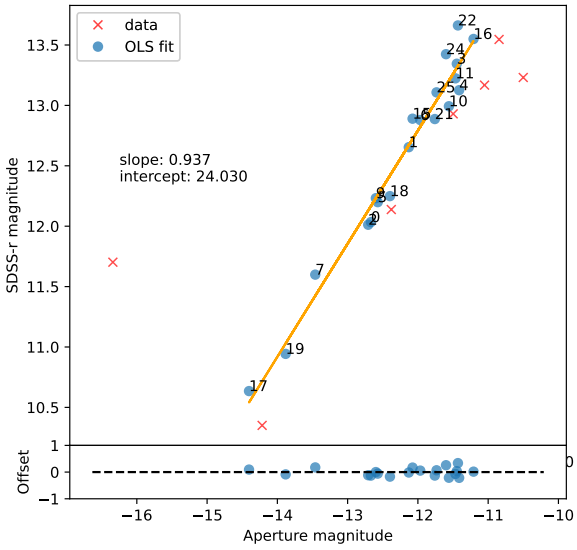

(a)

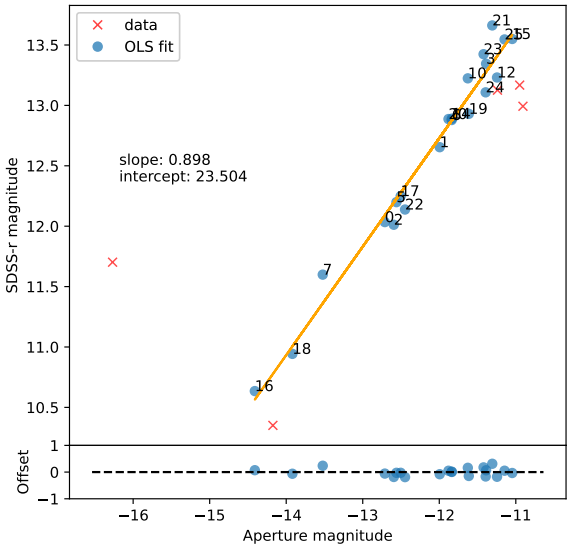

(b)

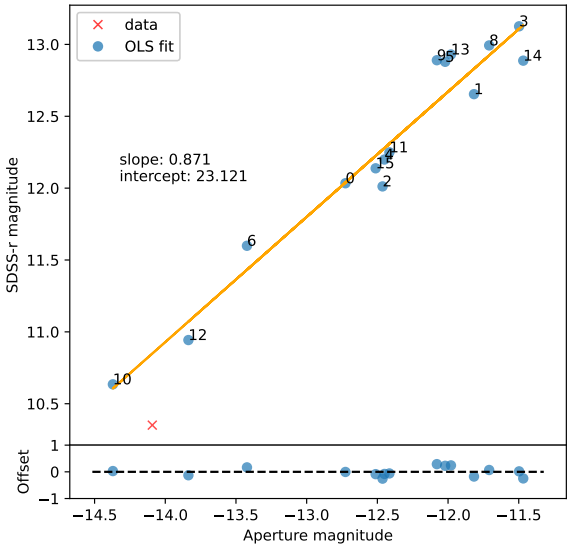

(c)

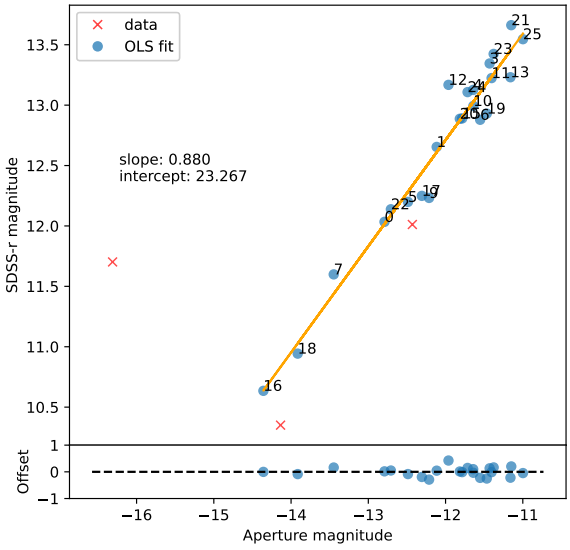

(d)

Figure 9. The aperture magnitude measured from DoA Dome Telescope in sdss-r band. The orange line shows the regression line, and the blue dots are the data. The red cross represents excluded data.

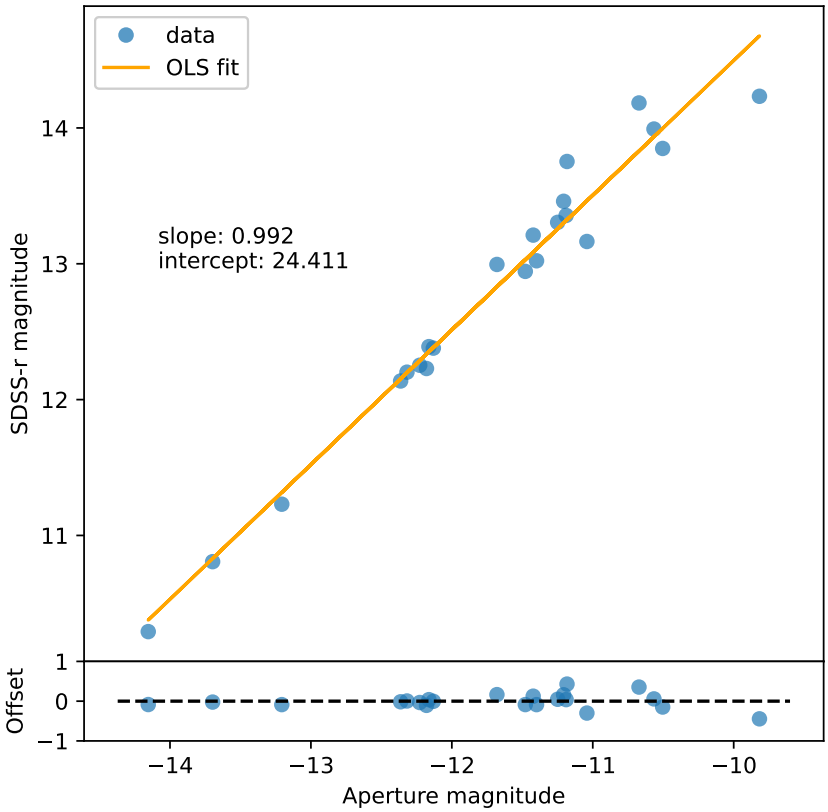

Figure 10. The flux calibration with reference catalog from SDSS. The result shows that the slope of the regression line is very close to 1, and the linear model is statistically significant with a p-value of 0.000, suggesting a satisfying zeropoint calibration.